Title

ELECTRICAL RESISTIVITY STUDIES OF UNIDIRECTIONALLY SOLIDIFIED Al-CuAl2 EUTECTIC ALLOY

Author

Danso, Kwaku Abiam.

Publication Date

1975-02-01

LBL-3547
c.1

ELECTRICAL RESISTIVITY STUDIES OF UNIDIRECTIONALLY SOLIDIFIED Al-$CuAl_2$ EUTECTIC ALLOY

Kwaku Abiam Danso
(M. S. thesis)

February 1975

Prepared for the U. S. Energy Research and Development Administration under Contract W-7405-ENG-48

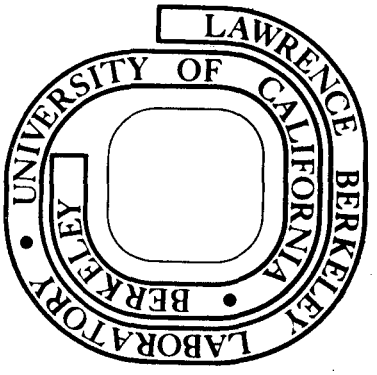

LBL-3547
c.1

DISCLAIMER

Table of Contents

ELECTRICAL RESISTIVITY STUDIES OF UNIDIRECTIONALLY SOLIDIFIED Al-$CuAl_2$ EUTECTIC ALLOY

Kwaku Abiam Danso

Inorganic Materials Research Division, Lawrence Berkeley Laboratory and Department of Materials Science and Engineering, College of Engineering; University of California, Berkeley, California

ABSTRACT

Experiments were conducted on the electrical resistivity of the Al-$CuAl_2$ eutectic and Al-5.7 Cu alloy, both as cast and directionally solidified, and aged at 25,150 and 315°C. Directional solidification produces an oriented microstructure and reduces the resistivity significantly. The resistivity of the quenched Al-5.7 Cu alloy is 4.65 μΩ-cm and this extends Nordheim's rule over the entire range of solid solubility of Cu in Al. Analysis of the data showed that use of independently measured component properties to calculate composite properties from the rule of mixtures is not justified even if the gross phase geometry is well defined.

I. INTRODUCTION

A. Objective

The present study was stimulated by the increasing number of structural applications of composite materials, such as the current interest in directionally solidified eutectics (in situ Composites) as promising candidate materials for turbine blades, and the possibility that in some systems materials having important electronic properties can be made.

A composite is a solid heterogeneous medium consisting of a mixture of several distinct phases separated by well defined interfaces. In this respect all multiphase alloy systems are composite materials, but in the context of this work composite is restricted to multiphase systems (usually two phase) consisting of an aligned reinforcing phase dispersed in a second matrix phase. Such composites can be made by artificial joining of two phases whose properties are complimentary.[1] However, composites can also be made by unidirectional solidification of eutectics from the melt.[2]

Considerable theoretical and experimental work has been done on the mechanical properties of both fabricated and in situ composites. It has been found that in composites having a regular aligned microstructure the mechanical properties of the composites can usually be predicted given the properties of the individual components and their volume fractions. What is most commonly used is the simple "Rule of Mixtures".

Theory predicts that the electrical properties such as conductivity and dielectric constant, and magnetic properties such as the magnetic

permittivity obey the same laws as for mechanical properties with appropriate substitutions in the relevant equations.[3] However, in contrast to the situation for mechanical and thermophysical properties very little experimental work has been done on electrical properties.

The primary objective of this study was to ascertain if the simple rule of mixtures holds for the electrical resistivity of in-situ composites with well aligned microstructures. The system chosen for study was the Al-Cu eutectic which has been solidified unidirectionally to produce lamellae of $CuAl_2(\theta)$ phase platelets parallel to the growth direction in a matrix of aluminum slightly alloyed with copper (κ phase). In the present work one of the phases, the Al-5.7 wt.% Cu alloy is itself a composite material, because upon solution heat treatment and aging, finely dispersed $CuAl_2(\theta)$ precipitates are formed in the Al matrix. Since the electrical properties of single crystals of this material have not been reported, and the electrical properties of $CuAl_2$ are also unknown, a second objective of this work was to determine the electrical properties of Al-5.7 wt.% Cu(κ) and $CuAl_2(\theta)$.

B. Properties and Applications of Composite Materials

1. Structural Applications

Among the most important properties of in-situ composites for modern applications are (a) the strengthening inherent in most eutectic composites--the load carrying capability of a stiff strong phase, either fibrous or lamellar, and (b) the stability of eutectic microstructures during long times at elevated temperatures.

In the recent rapid improvements in jet engines for speeds twice and thrice that of sound, one of the most demanding materials requirements has been for turbine blades in the hottest parts of the engine where service temperatures are up to 2300°F and the metal is subjected to high stresses in a highly oxidizing and corroding atmosphere. Present day turbine blade materials which operate at 1800° to 1900°F are Ni-base super alloys consisting primarily of nickel-rich solid solution (γ) hardened by ordered Ni_3Al rich (γ') particles (Ni-Ni_3Al, or γ-γ').[2] Some of these are directionally solidified to avoid transverse grain boundaries.

Alloy designers are now looking for new materials to operate at even higher temperatures. A class of materials under study is refractory metal alloys; e.g. alloys of molybdenum, tungsten and niobium. They, however, suffer from the disadvantage of rapid oxidation. Another class, ceramic materials, also suffers from brittleness. Thus many researchers are now investigating aligned eutectics as the most promising high temperature substitutes for current superalloys; the two major classes being those reinforced with TaC fibers, and those reinforced with Ni_3Nb (δ) lamellae.[2]

TaC Eutectics. TaC has the highest melting point of any substance known, about 7000°F, and an elastic modulus of over 60×10^6 psi. Starting with the Ni-TaC and Co-TaC eutectics, some workers[4] have improved matrix properties by adding various alloying elements, while retaining well-aligned TaC fibers. Cr and Al were added for strengthening and corrosion resistance. The Co-base-TaC eutectic has the highest

known creep resistance at high temperatures, but lacks an equivalent of γ' hardening and is therefore weaker than the Ni-base alloys at intermediate temperatures.

Measurements of high-cycle fatigue strengths and impact strengths, properties which are important for engine applications, have also shown that even after extensive fiber cracking (after straining) eutectics can show considerable strength and ductility.

Ni_3Nb (δ) Eutectics. One of the strongest eutectics so far developed is the Ni_3Al-Ni_3Nb (γ'-δ) lamellar eutectic. Two major drawbacks of this eutectic between two intermetallic compounds (γ'-δ) however are the limited ductility at low temperatures and limited oxidation resistance. To correct these weaknesses alloying modifications, including post-solidification heat treatments and the additions of Al and Cr to produce γ' precipitation within the γ phase to improve oxidation resistance have been made.[2] The γ,γ',δ eutectic showed improved low temperature ductility with only moderate loss in creep strength compared to γ'-δ eutectic, and promises to be a good turbine-blade material.

As stated earlier, the stability of eutectic microstructures during aging at elevated temperatures is one of the major advantages of eutectics. Reference (2) cites some work on two aspects of thermal stability--the effect of the thermal cycling and of temperature gradients Further work is needed in this area, but the indications are that eutectics, which are known to reach a limiting coarseness in microstructure after prolonged aging will have superior properties in these respects.

2. Non-structural Applications

While the major potential applications for in-situ composites seem to be those requiring good mechanical and thermo-physical properties, these materials also have interesting and potentially important electrical, magnetic, and optical properties.[5]

a. Semiconducting materials. The aligned InSb-NiSb eutectic contains long conducting rods of NiSb dispersed in a semiconducting InSb matrix.[5,6] It exhibits a large magnetoresistive effect, and Siemens markets magnetic field sensors, current transducers, contactless potentiometers and switches based on this property. The aligned InSb-NiSb eutectic also acts as an infrared detector which operates at room temperature with a biasing magnetic field, giving a detectivity figure, D^*, of 2×10^7 Watts^{-1}sec$^{-1/2}$, and a sensitivity to 15 μm with modulation frequencies at several KHZ. In another application the material has been used as a source of light in the visible and infrared spectral regions. Apparently the radiation in this case results from the recombination of injected charge carriers.

Another in-situ composite with a large magnetoresistive effect is the Cd_3As_2-NiAs eutectic studied by Elliot and Hiscocks.[7] In spite of its high carrier concentration (10^{18}cm^{-3}) at room temperature, it has a high mobility (15,000 cm^{2}v^{-1}sec^{-1}) at room temperature which increases down to 4°K. However the magnetoresistive effect is not as large as in the InSb-NiSb eutectic. Rod-like morphologies were obtained in the above cases. In another instance controlled solidification of the SnSe-$SnSe_2$ eutectic produced a material with alternating N and P type semiconducting lamellae.[8]

b. Superconducting eutectic materials. It is anticipated that if eutectics containing fine superconducting rods in non-conducting matrices can be produced, they will be able to produce high magnetic fields. Attempts have been made to obtain very high field superconducting eutectics. Studies have shown that enhanced critical fields (greater than that expected for the pure phases) were exhibited by type I, Pb-Cd, Pb-Sb,Sn-Bi, Sn-Zn, and Sn-Cd eutectics.[5] However, Livingston[9] has shown that this increase in critical fields may be due to the presence of solid solution in the terminal phases which would be expected to make them Type II (high field) materials.

c. Optical eutectic materials. The NaCl-NaF, NaCl-LiF, and NaBr-NaF halide eutectics have been studied, with the NaF-NaCl giving the most satisfactory results.[10] It was found that image transmission properties similar to those of fiber optic materials were obtained along an NaF-NaCl eutectic ingot when the growth conditions were carefully controlled so the axes of NaF rods were parallel to the ingot axis. The controlled eutectic was in addition found to be a far-field infrared transmitting medium for wavelengths longer than the inter-rod distance.

d. Ferromagnetic eutectic materials. Many studies have been conducted on ferromagnetic eutectic systems, mostly with the objective of increasing the coercive force. By decreasing the size of iron rods in a non-magnetic matrix to that of a single domain the coercive force should be very large. Several workers have been cited in Reference 5, including Albright, et al.[11] on the Fe-FeS eutectic,

Galasso, et al.[12] on the Fe-Fe_xSb eutectic, and Livingston[13] on the Co-Au eutectic. A high speed solidification technique was developed which enabled Cline and Livingston to produce rods much smaller in diameter than the micron sizes obtained by normal solidification techniques used in earlier studies.[14] An intrinsic coercive force of 330 oersteds, (and 925 oersteds by subsequent wire drawing) were obtained. Other systems of such eutectics studied include Fe-Fe_2Ti, Fe-$FeBe_2$, Fe-Fe_2Zr, and FeCo-FeCoB (Ref. 40 of (5); Heimke, U.S. Patent 3,434,892 (1965)). Details were not given by the author.

II. THEORY

The different kinds of eutectic alloys, their microstructures, modes of growth and the theories and properties of lamellar as well as non-lamellar eutectic alloy solidification have been discussed by Chadwick,[15] as well as other workers, references (16-38).

Theories of the electrical orelectronic conduction in metals and alloys have been well treated by several workers.[39-54] Those relevant to a general understanding of electrical resistivity in alloys, and in changes during aging treatments are summarized here.

A. Effect of Alloying Elements and Impurities on Resistivity

If the temperature of a sample of a dilute solid solution is reduced, its resistivity decreases but does not approach zero at absolute zero of temperature; it approaches a limiting residual value. This was expressed in a rule by Matthiessen[39] that in such metals the total resistivity ρ is the sum of the temperature-dependent resistivity ρ_T (the ideal resistance) of the pure metal, and a temperature independent or residual resistivity ρ_R, i.e.

$$\rho = \rho_R + \rho_T \quad \text{(Matthiessen's Rule)} \tag{1}$$

This implies that the foreign atoms do not alter the effective number of free electrons or the energy band structure or the characteristic temperature of the metal, and their thermal vibrations scatter the electrons in the same way as those of the parent metal. The effect of

copper atoms on the resistivity of aluminum is shown in Fig. 1.

The residual resistivity ρ_R is due solely to chemical and physical imperfections while ρ_T arises solely from the thermal vibrations of the ideally pure and perfect crystal lattice. The scattering of electrons by the impurities or alloying and the resultant increase in ρ results from the disturbance of the lattice, but the effect may arise in several ways:

(1) It may occur because of the heterovalency of the impurity atom. An atom of higher valency than the solvent atom causes "Screening" of the foreign ion by the remaining conduction electrons.

(2) If the solute atom is homovalent with the solvent metal (e.g. P in Na, or Ag in Cu), no charge difference exists, but scattering occurs in two ways:

   (a) The scattering cross section of the solute may differ from the parent metal;

   (b) because of the size factor of the solute atoms the matrix may be locally strained by the impurity, and this displacement of the ions will give rise to electron scattering.

(3) The formation of a new phase will increase the scattering; significant scattering would occur for either coherent or incoherent precipitation.

For the case of a completely disordered alloy of metals A and B, the dependence of ρ_R on a single impurity has been worked out by Nordheim[41] and is given by

$$\rho_R(x) \propto x(1-x) \quad \text{(Nordheim's Rule)} \qquad (2)$$

where x is the atomic concentration of metal A and (1-x) that of metal B. For dilute solutions ($x \ll 1$) Eq. (2) becomes

$$\rho_R \propto x \tag{3}$$

which agrees with the plot of Fig. 1.

The generalized rules for the relationship between electrical resistivity and the constitution of alloys are sometimes called Le Chatelier-Guertler Rules:[40]

(1) In heterogenous mixtures of two phases, the electrical resistivity varies linearly if the composition is given in volume precent. Different cases between pure metals and intermediate phases are given with illustrative figures in Ref. 40. ρ for intermediate phases is always higher than the value calculated using the Rule of Mixtures.

(2) Intermetallic compounds in the case of two electropositive metals usually have a resistivity which does not differ greatly from that of the pure constituent metals though it is invariably greater than that of the constituent of lower ρ. (Ref. 42, p. 95)

(3) In solid solutions ρ is always higher than that of the solvent metal and is usually higher to a considerable degree if the composition is given in volume percent.

B. Variation of Electrical Resistivity During Precipitation and Age Hardening

The structures of the different precipitates formed in the age hardening of dilute Al-Cu alloys together with hardness versus aging curves are described by Hayden et al.[43] and by Hardy and Heal.[45] The size and distribution of the precipitated particles and their orientation relationships with the matrix have varying effects on the properties of the metal or alloy. In the Al-Cu system illustrated in the above references for Al-4%Cu, the first precipitates to form are dispersed disc-like clusters of Cu atoms of 2 to 3 atoms (10Å) thick and 100Å total length called G-P-1 zones. These are coherent with the matrix and oriented on the {100} Al planes.

The next precipitates, G-P-2 zones, are disc-shaped tetragonal structures of 1500Å diameter and 150Å thick, coherent along the diameter, and incoherent along the thickness, with average composition $CuAl_2$. The G-P-2 zones produce the maximum in the hardness curve due to the shear and compressive strains so produced.

The next precipitate to form, the θ' - zone is similar to the $CuAl_2$ but dislocation loops around the precipitates destroy the coherency, eliminates the long range elastic forces and lead to a softening.

The final equilibrium precipitate to form is the θ zone, body centered tetragonal $CuAl_2$, non-coherent with the matrix, with lattice parameters a=6.054Å, c=4.864Å and 12 atoms in the unit cell.[46]

Just as the precipitation phenomenon is known to cause a maximum in hardness during aging, the resistivity curve also has a maximum during aging,[40,47] due to the formation of different sizes and structures of precipitates and their different scattering effects on conduction electrons.

Three theories have been proposed to account for the resistivity maximum in the Al-Cu system, as in other system.[48] These are due to Mott, Geisler and Fine respectively. Mott suggested that the maximum occurred when the cluster size reached a critical value equal to the wavelength of the conduction electrons (about 10Å) at the Fermi level, since the clusters would then cause strong scattering.[49]

A. H. Geisler[50] suggested that the peak was due to coherency strains occurring in the GP zones in Al-Cu. M.F. Fine[51] suggested that the increase in resistivity in Al-Cu might be due to the presence of a large number of structural dislocations around GP-zones due to the difference in atomic diameters (Al=4.05Å, Cu=3.62Å).

Since the resistivity maximum has been shown to occur in alloys where the zones are spheres, plates and needles, and is not dependent on coherency strains between the zone and matrix, only Mott's theory of critical cluster size appears the most plausible; this is supported by some experiments of Herman and Cohen.[52] These authors showed by doing x-Ray small angle scattering experiments on aged Al-5.3 at.% Zn that the resistivity maximum corresponded to clusters of size about 10Å.

C. The Rule of Mixtures for a Lamellar Composite

The conductivity, dielectric constant and magnetic permittivity are all dependent upon the entire statistics of the phase geometry of a material, just as the elastic properties are known to depend on phase geometry. Several cases have been treated and illustrated by Hashin.[3] For the case of a lamellar two phase composite such as the Al-$CuAl_2$ eutectic system studied, (for which the ideal microstructure is illustrated in Fig. 2) the equations for the resistivity in the longitudinal (with respect to growth direction) and transverse directions reduce to

$$\frac{1}{\rho_{c_{\parallel}}} = \frac{v_\theta}{\rho_{\theta_{\parallel}}} + \frac{(1-v_\theta)}{\rho_\kappa} \quad \text{(longitudinal)} \tag{4}$$

or

$$\sigma_{c_{\parallel}} = \sigma_{\theta_{\parallel}} v_\theta + \sigma_\kappa (1-v_\theta)$$

and

$$\rho_{c_\perp} = \rho_{\theta_\perp} v_\theta + \rho_\kappa (1-v_\theta) \quad \text{(transverse)} \tag{5}$$

where

$\rho_{c_{\parallel}}, \rho_{c_\perp}$ = resistivity of the lamellar eutectic (Al-33 wt.% Cu) in the longitudinal and transverse directions, respectively.

$\rho_{\theta_{\parallel}}, \rho_{\theta_\perp}$ = the resistivity of the $CuAl_2(\theta)$ phase in the longitudinal and transverse directions respectively.

ρ_κ = the resistivity of the κ phase.

v_θ, $(1-v_\theta)$ = the volume fractions of the θ and κ phases respectively.

The κ phase is cubic and hence its conductivity is isotropic. However in the Al-$CuAl_2$ eutectic, the θ phase is body centered tetragonal. Thus it is expected that $\rho_{\theta_{\parallel}}$ and $\rho_{\theta_{\perp}}$ will differ.

Given values of ρ_c, ρ_θ, ρ_κ and v_θ, a test of the Rule of Mixtures is straightforward. However, an alternative test can be made if ρ_c and ρ_κ can be determined separately, v_θ is known, and if ρ_θ is not a function of aging time and relatively independent of aging temperature. Thus, e.g. using the results of measurements of $\rho_{c_{\parallel}}$ and ρ_κ at temperature T_1, Eq. (4) can be used to calculate $\rho_{\theta_{\parallel}}$. If Eq. (4) holds, the value of $\rho_{\theta_{\parallel}}$ thus obtained can be combined with direct measurements of ρ_κ to predict the value of $\rho_{c_{\parallel}}$ at temperature T_2. Similar considerations apply to the transverse case.

III. EXPERIMENTAL

A. Materials Preparation and Characterization

Starting materials of 99.999% purity were use to prepare the alloys. Five Al-33.3 wt.% Cu eutectic alloys were prepared by unidirectional solidification using an open horizontal graphite boat (L=17 cm, W=1.9 cm, H=1.25 cm) under argon atmosphere in a quartz tube. The as cast alloys were melted and homogenized in the liquid phase at about 870°C in a tube furnace whose temperature profile had a gradient of about 27°C/cm at the eutectic temperature. The apparatus is described in Refs. 37 & 38. Freezing rates (assumed equal to the rate of furnace travel) in the range 1.4 to 23 cm/hr were used. It was determined that the profiles with and without boat and charge of alloy were different and the former was used to measure the temperature gradient at the liquid-solid interface. Later a ceramic boat (inside dimensions: L=24 cm, W=2.0 cm, H=1.4 cm) was used to grow two eutectic alloys and two of Al-5.7 wt.%Cu.

After solidification each sample was polished on a 240 Grit belt sander and on 240, 320, 400 and 600 Grit SiC polishing papers and then on a 0.5 micron Al-Silica cloth on a polishing wheel. The eutectic was etched with Keller's reagent (10 ml HF, 25 ml HNO_3, 15 ml HCl, 50 ml H_2O) at room temperature. The Al-5.7 wt% Cu was etched by immersing in a solution of 25 ml HNO_3 (conc.), 75 ml H_2O for 60 seconds at 70°C, quenched in cold water and then in another solution of 0.5 g·NaF, 1.0 ml HNO_3(conc.), 2.0 ml HCl (conc.) and 97.0 ml H_2O for 15 to 30 seconds, and washed in warm running water. The samples were first polished in the full ingot shape to observe the structure with the unaided eye and then

with the optical microscope. Then they were sectioned longitudinally and transversely to reveal the microstructure parallel to the growth direction (faces A and C) and transverse to the growth direction (Fig. 3). Microphotographs were taken at various positions, and the interlamellar spacings λ for each eutectic were measured for each growth rate R.

B. Aging and Resistivity Measurements

Specimens were sectioned from large grains of the ingots of both the eutectic and the Al-5.7 wt% Cu alloy. Materials used for electrical measurements were cut from alloys grown at 4.6 cm/hr and cut in the form of rectangular parallelepipeds of approximate dimensions: length (L)=4 cm, width (W)=5mm, thickness (T)=1 mm. The exact dimensions of each specimen were used in calculating ρ.

The heat treatment and aging equipment consisted of air resistance furnaces with constant temperature controllers ($\pm$ 5°C). A chromel-alumel thermocouple was inserted through an opening in the furnace door and connected to a thermocouple temperature indicator reading directly in degrees C. A bucket of water directly under the furnace was used as a quench bath.

The four probe resistivity measuring apparatus consisted of a regulated current source, in series with a 2 ohm resistor, an ammeter, and a millivolt potentiometer with a sensitivity of about 5 μv per slidewire division. A current of 2 amps was used, and the voltage measured. Higher currents were found to heat the specimen and give unsteady readings.

For the solution heat treatments all specimens were sealed in a stainless steel envelope and homogenized at 530±5°C for 1 hour and quenched to room temperature. They were then alternately aged at the selected temperatures and quenched for resistivity measurements at room temperature.

To facilitate measurements with the small size samples, a device was designed to hold the specimen such that the current passed perpendicular to the specimen edge through a spring loaded copper connector. The voltage contacts were sharp pointed tungsten connected through spring loaded copper terminals to the potentiometer.

Curves of resistivity versus aging times were plotted for the data obtained at 315°C, 150°C and room temperature (25°C) on the directionally solidified eutectic and Al-5.7% Cu, and at room temperature only for the polycrystalline Al-5.7% Cu and eutectic specimens.

C. Transmission Electron Microscopy

Thin films of the unidirectionally solidified Al-$CuAl_2$ eutectic were prepared by cutting 0.020 in. sections of material perpendicular to the growth direction. They were mechanically polished to about 0.008 to 0.010 in., cleaned in a solution of 35% H_3PO_4, 10%NHO_3 and 55% H_2SO_4 at 60°C and electrochemically polished in a solution of 817 cc H_3PO_4, 134 cc H_2SO_4, 156 gm CrO_3 and 40 cc water at 75°C, using an aluminum cylindrical cathode and 10-12 applied volts. Bright field images and selected area diffraction patterns were taken using a Siemens 100 KV Transmission Electron Microscope.

IV. RESULTS

As expected from previous work an aligned lamellar microstructure is obtained when the eutectic alloy is frozen unidirectionally under appropriate conditions. Typical optical micrographs are shown in Fig. 4(a) and 4(b). Occasional faulting of the lamellae is observed but the microstructures are a reasonably good approximation to the model shown in Fig. 2. Microstructures of the Al-5.7% Cu alloy are shown in Figs. 5(a),(b) and (c). Copious precipitates of θ are seen; but whereas no platelike morphology is apparent in the as cast alloy (Fig. 5(a)), the unidirectional solidification under the conditions used to grow the eutectic alloy has clearly produced oriented precipitates, Fig. 5(b) and 5(c). Furthermore, since precipitation of θ platelets occurs on {100} in the κ phase it can be concluded that under these conditions the growth direction is approximately $\langle 100 \rangle$, and the normal to the platelets is $\langle 011 \rangle$. An electron photomicrograph of the eutectic grown at 4.6 cm/hr is shown in Fig. 6. The regions of the θ platelets are densely covered with small spots of low contrast. No attempt was made to identify these spots. The width of the κ regions is about 1.8 μm and in contrast with the separately grown Al-5.7 Cu alloy, no well defined θ precipitate morphology can be seen. As shown in Fig. 7(a), electron diffraction patterns of the κ phase confirm the assignment of $\langle 100 \rangle$ growth direction for this phase and $(011)_\kappa$ parallel to the lamellae. However the θ phase is difficult to thin and in this work only kikuchi patterns, such as shown in Fig. 7(b) could be obtained.

At this writing these patterns have not been analyzed. The only clear conclusion to be drawn is that the growth direction for the θ platelets is not ⟨001⟩.

While resistivity studies were conducted only on materials grown at one growth rate, some additional runs were made at several others. As shown in Fig. 8 the expected $\lambda^2 R$ = constant relationship was found.

The results of experiments conducted to determine the effects of unidirectional solidification on electrical resistivity are shown in Fig. 9. Comparison of the curves for polycrystalline and directionally solidified material shows that the resistivity of both the κ and θ phases are reduced significantly. The extent and degree of the decrease is largest for the κ phase. Since the precision of the measured resistivity data are about ± 0.05 μΩcm the effect in both instances is clearly outside experimental error.

Data obtained for the resistivity changes in the directionally solidified alloys during aging are shown in Figs. 10, 11 and 12. As stated earlier the data are accurate to about ±0.05 μΩcm, and to this approximation it appears that the curves for the eutectic and the κ phase follow the same trends at all temperatures and aging times. A weak maximum at about 20 hours is apparent in the data obtained at 25°C and possibly there is one at about 8-10 hours for the 150°C aging.

The resistivity of all Al-5.7 Cu alloys have an initial value whose average is 4.60±0.05 μΩcm at 25°C. No previous data have been reported for this composition. However, as shown in Fig. 1 this result compares well with data obtained by previous workers using smaller alloying

additions of Cu to Al. By extrapolation Nordheim's rule is thus extended to the limit of solid solubility in the Al rich end of the Al-Cu equilibrium diagram.

The curves for $\rho_{\theta_{\parallel}}$ calculated using Eq. (4) and $v_{\theta}=0.4$ [38] indicate values of 8.2 and 8.3 μΩcm for 25° and 150°C aging, respectively, whereas the limiting calculated value approaches 9.9 μΩcm for the data obtained at 315°C aging. While the differences in the first two instances maybe due to experimental error, the calculated value at 315°C must be attributed to other causes.

The resistivity data at 315°C for the Al-5.7 Cu alloy and the eutectic begin at the same values as those obtained at 25 and 150°C, but decrease rapidly, appear to reach a maximum at about 2-3 hours and thereafter undergo relatively little change. The value calculated for $\rho_{\theta_{\parallel}}$ increases, reaching a limiting value of 9.9 μΩcm.

V. DISCUSSION AND CONCLUSIONS

The applicability of the simple rule of mixtures depends upon the extent to which variations in local material properties, and phase geometry can be ignored.[3] This is clearly borne out by the data shown in Fig. 9. Directional solidification has produced a significant reduction in the resistivity of the κ alloy, and since the microstructures in Figs. 5(a), 5(b) and 5(c) show a marked change from globular to oriented precipitates it is clear that specification of the composition is inadequate even for what appears to be "statistically isotropic" material.

The data in Fig. 9 which compares the resistivity of polycrystalline eutectic alloy with the lamellar eutectic are more difficult to interpret. The data for the polycrystalline eutectic are complicated by the fact that the massive θ precipitate takes up all orientations equally and hence the contributions of this phase are a weighted average of ρ_{θ_A} and ρ_{θ_c}. Second, the microstructure shown in Fig. 6 shows that the precipitate morphology obtained in the κ portions of the eutectic occurs on a much finer scale than in the separately grown κ alloy, and does not appear to be crystallographic on any extended scale. In short the data for the resistivity of the κ phase which should have been inserted into Fig. 4 may well be in error. Since the value of ρ_κ could be as large as 5.1 μΩcm, the estimate of $\rho_{\theta_{||}}$ could be as small as 6.8 μΩcm. In this respect the estimates of $\rho_{\theta_{||}}$ must be taken as upper limits.

The dependence of the calculated value of $\rho_{\theta_{\parallel}}$ on temperature cannot be interpreted as compositional. As shown in Fig. 13 the θ phase in the Al-Cu phase diagram is an intermediate compound in which the resistivity is expected to be dependent upon composition. However, in the range of aging temperature studied in this experiment the phase boundary is almost vertical, the total change of composition of the θ phase is less than 0.1%. The kinetic changes in ρ_K represent a change from quenched Al-5.7 Cu to that of an alloy composed of a solid solution of Al and Cu of varying compositions ranging from 5.7 W% Cu down to 0.6 W% Cu, with the excess 5.1 Cu present in the matrix as θ precipitates.

The volume fraction assigned to the θ phase is based upon results obtained by slow cooling to room temperature from the eutectic temperature. However, the data obtained by aging at 315°C should really compare the resistivities of the composite of Al-0.6 Cu for which $\rho_K \sim 2.6$ μΩcm (Fig. 1); and a larger volume fraction of lamellar θ precipitate. Thus the apparent change in resistivity of $\rho_{\theta_{\parallel}}$ with aging temperature is probably an over estimate. The results obtained in this experiment thus do not test the simple rule of mixtures, Eq. 4. Furthermore, in view of the effect of microstructure on the resistivity of the Al-5.7 Cu alloy already discussed the rule would not have been tested even if separate measurements on $CuAl_2$ (θ) single crystals were available. The present work emphasizes the great importance of phase geometry and the possible errors inherent in attempting to calculate composite properties.

ACKNOWLEDGEMENTS

It is a pleasure to acknowledge the help of Lee Johnson for Metallographic work, Tom Mowles and Julian Patenaude for general technical assistance, Margaret Robson for assistance with the Transmission Electron Microscopy work, Walt Toutolmin for the design of the four probe electrical measurement device, Lois Fernander, Alice Ramirez, Shirley Ashley and Jean Wolsgel for the typing work, Gloria Pelatowski for the preparation of the graphs and Doug Kreitz for the photographic work.

Special thanks go to the members of the thesis committee, Professors M.F. Merriam, W.G. Oldham for helpful comments, and especially to my thesis advisor, Professor R.H. Bragg for all the time he spent working with me on this project.

This work was supported by the United States Atomic Energy Commission through the Inorganic Materials Research Division of the Lawrence Berkeley Laboratory.

REFERENCES

1. A.G. Guy, Introduction to Materials Science, McGraw Hill Book Co., U.S.A. (1972).
2. J.D. Livingston, Lakeville Conference on In-Situ Composites; General Electric Tech. Info. Ser., No. 72CRD 276, Oct. 1972, Schenectady, New York.
3. Z. Hashin, Theory of Composite Materials, Ceramic Microstructures, R. Fulrath and J. Pask, Ed., Wiley & Sons, New York (1966), 333.
4. H. Bibring, G. Seibel, and M. Rabinovitch, Mem. Sci. Rev. Met. 49, 341 (1972).
5. F.S. Galasso, F.C. Douglas, and J.A. Batt, J. Metals 22, No. 6 40 (1970).
6. H. Weiss, Met. Trans. 2, 1513 (1971).
7. C.T. Elliot, S.E.R. Hiscocks, On the Electrical and Magnetosesistance Properties of Cd_3As_2-NiAs, Brit. J. Appl. Phys. (J. Phys. D), Vol. 2, 1083 (1969).
8. W. Albers and J. Verbekt, The SnSe-$SnSe_2$ Eutectic-A P-N Multilayer Structure, (Ref. 27 of 5 above).
9. J.D. Livingston, Superconducting Properties of Eutectics, J. Appl. Phys. 38, No. 5, 2408 (April 1967).
10. J.A. Batt, F.C. Douglas and F.S. Galasso, Optical Properties of Unidirectionally Solidified NaF-NaCl Eutectic, Amer. Cer. Soc. Bulletin, Vol. 48, 622 (1969).

11. D.L. Albright, G.P. Conrad II, and R.W. Kraft, Magnetic Behavior of Eutectic Alloy, Featuring an Aligned Array of Iron Rods, J. Appl. Phys. 38, No. 7, 2919 (1967).

12. F.S. Galasso, F. Douglas and J. Batt, Characterization of the Fe-Fe_xSb Eutectic System with Respect to Structure and Ferromagnetic Properties, J. Appl. Phys. Vol. 38, 3241 (1967).

13. J.D. Livingston, Structure and Magnetic Properties of Au-Co Aligned Eutectic, General Electric Tech. Info. Ser. No. 69-C-255, 1969.

14. H.E. Cline and J.D. Livingston, High Speed Directional Solidification of Sn-Pb Alloys, Gen. Electric Tech. Info. Ser., No. 69-C-083, (1969).

15. G.A. Chadwick, Eutectic Alloy Solidification, Prog. Mat. Sci. Vol. 12, No. 2 (1963).

16. A.S. Yue, Microstructure of Magnesium-Aluminum Eutectic, Trans Met. Soc. AIME 224, 1010 (1962).

17. G. Tamman, A Textbook of Metallography (1925), Translation into English, The Chem. Cat. Co., New York.

18. W. Rosenhain and P. Tucker, Phil. Trans. 209A, 89 (1909).

19. R. Vogel, A. Anorg. Chem. 76, 425 (1912).

20. F.E.E. Lamplough and J.T. Scott, Proc. Royal Soc. 90A, 600 (1914).

21. W. Straumanis and N. Brakss, Z. Phys. Chem. 30B, 117 (1935).

22. W.A. Tiller, Liquid Metals and Solidification, A.S.M. Cleveland, Ohio (1958).

23. P.G. Shewmon, Transformations in Metals, McGraw-Hill, Inc. New York (1969).

24. C. Zener, Trans. Amer. Inst. Min. (Metal) Engrs. 167, 550 (1946).

25. E.C. Elwood and K.Q. Bagley, J. Inst. Met. 76, 631 (1949).

26. N. Takahashi, J. Appl. Phys. 31, 1287 (1960).

27. R.W. Kraft, Trans. Met. Soc. AIME 224, 65 (1962).

28. A.S. Yue, F.W. Crossman, A.E. Vidoz and M.I. Jacobson, Controlled Microstructures of Al-$CuAl_2$ Eutectic Composites and their Compressive Properties, Trans. Met. Soc. AIME 242, 2441 (1968).

29. B.E. Sundquist and L.F. Mondolfo, Trans. Met. Soc. AIME 221, 607 (1961).

30. B.E. Sundquist and L.F. Mondolfo, Trans Met. Soc. AIME 221, 157 (1961).

31. R.W. Kraft and D.L. Albright, Crystallographic Substructures of Lamellar Al-$CuAl_2$ Eutectic, Trans Met. Soc. AIME 224, 1176 (1962).

32. G.A. Chadwick, J. Inst. Met. 91, 169 (1963).

33. J.D. Hunt and J.P. Chilton, J. Inst. Met. (1963). (Ref. 38 of 15.)

34. R.W. Kraft and D.L. Albright, Microstructure of Unidirectionally Solidified Al-$CuAl_2$ Eutectic, Trans. Met. Soc. AIME 221, 95 (1961).

35. J.P. Chilton, and W.C. Winegard, J. Inst. Met. 89, 162 (1961).

36. J.W. Rutter, Liquid Metals and Solidification, p. 243 ASM, Cleveland, Ohio (1958).

37. K. Ankra, M.S. Thesis, Dec. 1972, Unidirectional Solidification of Al-$CuAl_2$ Eutectic, University of California, Berkeley.

38. L.J. Salmon, M.S. Thesis, Experimental Techniques for Growing Unidirectionally Solidified Oriented Eutectics, University of California, Berkeley, June 1973.

39. A. Matthiessen and C. Vogt, Ann. Phys. Chem. (Pogg) 122, 19 (1864).

40. J.K. Stanley, Electrical and Magnetic Properties of Metals, Amer. Soc. for Metals; Metals Park, Ohio, 1963.

41. L. Nordheim, Ann d. Physik, 9, 641 (1931).

42. N.F. Mott, and H. Jones, The Theory of the Properties of Metals and Alloys, Dover Public, New York, 1958.

43. H.W. Hayden, W.G. Moffatt, and J. Wulff, The Structure and Properties of Materials, Vol. III Mechanical Behavior, John Wiley and Sons, New York (1966).

44. L.F. Pease, R.M. Rose, and J. Wulff, The Structure and Properties of Materials, Vol. IV: Electronic Properties; John Wiley and Sons, New York (1966).

45. H.K. Hardy and T.J. Heal, Report on Precipitation, Prog. in Met. Phys. 5, 143 (1954).

46. Lucio F. Mondolfo, Metallography of Aluminum Alloys, Wiley & Sons, New York, 1943.

47. W.L. Fink, D.W. Smith and L.A. Wiley, Age-Hardening of Metals, A.S.M., Metals Park, Ohio (1939), 31.

48. A. Kelly and R.B. Nicholson, Precipitation Hardness, Prog. Mat. Sci. 10, No. 3, 149 (1963).

49. N.F. Mott, discussion of paper by M.L.V. Gaylor, The Theory of Age Hardening of Metals, ASM., Metals Park, Ohio (1939), 31-53.

50. A.H. Geisler, Phase Transformations in Solids, p. 387, Wiley & Sons, 1951.

51. M.E. Fine, Acta. Met. 7, 228 (1959).

52. H. Herman and J.B. Cohen, Nature, 191, 63-64 (1961).

53. A.L. Norbury, Trans. Farad. Soc. 16, 570 (1921).

54. J.O. Linde, Ann d. Physik, 10, 52 (1931); 14 353 (1932); 15 219 (1932).

55. J.D. Livingston, Magnetization of Superconducting Cu-Pb Alloys, J. Appl. Phys. 39, No. 8, 3836 (July 1968).

56. M.R. Jackson, R.N. Tauber, and R.W. Kraft: Magnetic Anisotropy of MnSn-Sb Aligned Eutectic, J. Appl. Phys. 39, No. 9, 4457 (Aug. 1968).

57. F.S. Galasso, F. Douglas and J. Batt, J. Met. 22, No. 6, 40 (1970).

FIGURE CAPTIONS

Fig. 1. Effect of Cu additions on the electrical resistivity of Al (from Ref. 40).

Fig. 2. Ideal microstructure of a two-phase lamellar composite.

Fig. 3. Schematic designations of faces in frozen ingot. Faces A and C = longitudinal, Face B = transverse.

Fig. 4a. Longitudinal view (Face A) of unidirectionally solidified Al-$CuAl_2$ lamellar eutectic. Growth direction parallel to lamellae. Arrow direction = direction of current flow. Growth rate R = 1.4 cm/hr.

Fig. 4b. Transverse view (Face B) of same alloy as (a). Growth direction perpendicular to picture.

Fig. 5a. Structure of as cast polycrystalline Al-5.7 wt.% Cu showing formation of $CuAl_2(\theta)$ precipitates in the Al-rich (κ) phase. Magnification 2000×.

Fig. 5b. Longitudinal view of unidirectionally solidified Al-5.7 wt.% Cu. Growth direction left to right. Magnification 2000×.

Fig. 5c. Transverse view of same alloy as (b). Growth direction perpendicular to picture. Magnification 2000×.

Fig. 6. Bright field transmission electron microscope picture of Al-$CuAl_2$ lamellar eutectic. Transverse view--growth direction normal to picture.

Fig. 7a. Selected area diffraction pattern taken from Al-rich (κ) phase of Al-$CuAl_2$ eutectic with the Siemens transmission electron microscope.

Fig. 7b. Kikuchi pattern taken from $CuAl_2(\theta)$ phase of the Al-$CuAl_2$ lamellar eutectic.

Fig. 8. Variation of interlamellar spacing (λ) with growth rate (R).

Fig. 9. Electrical resistivity vs aging curves at 25°C showing effect of unidirectional solidification on ρ for Al-5.7 wt.%Cu (κ) and Al-33.3 wt.%Cu.

Fig. 10. Electrical resistivity vs aging curve at 25°C.

Fig. 11. Electrical resistivity vs. aging curve at 150°C.

Fig. 12. Electrical resistivity vs. aging curve at 315°C.

Fig. 13. Al-Cu pseudobinary phase diagram.

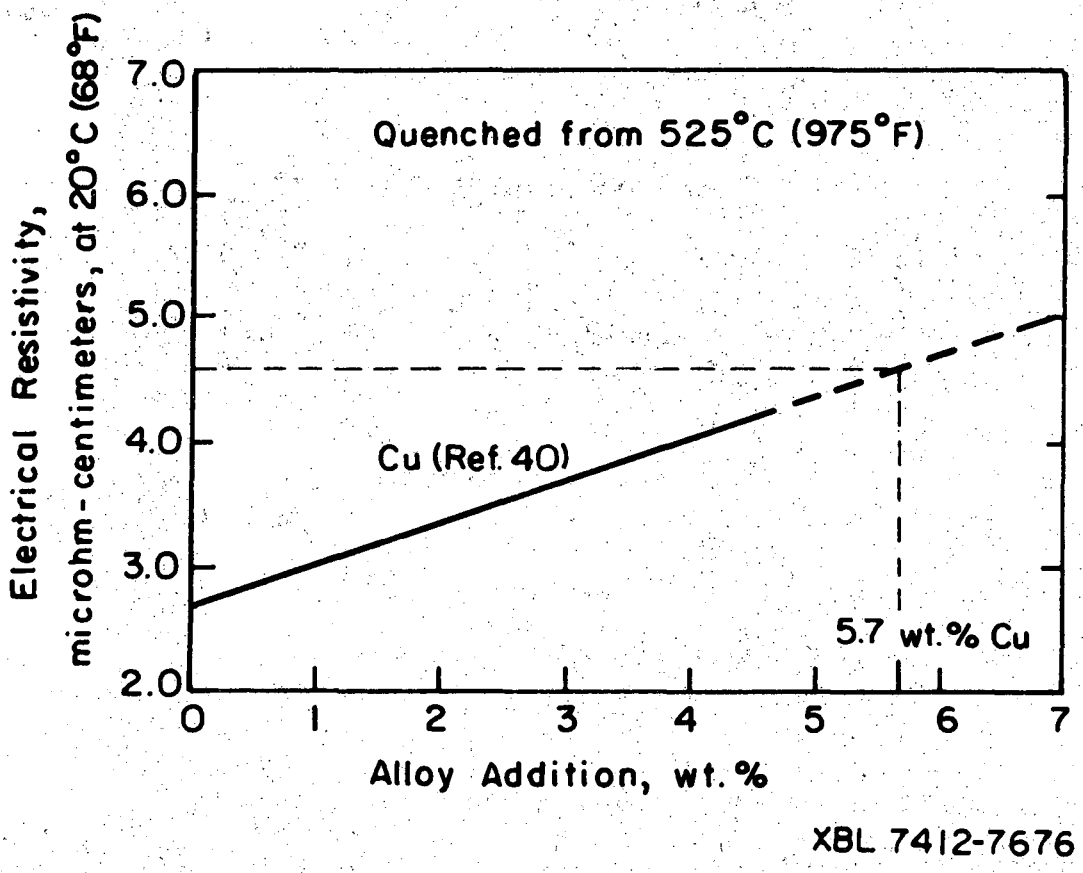

Fig. 1

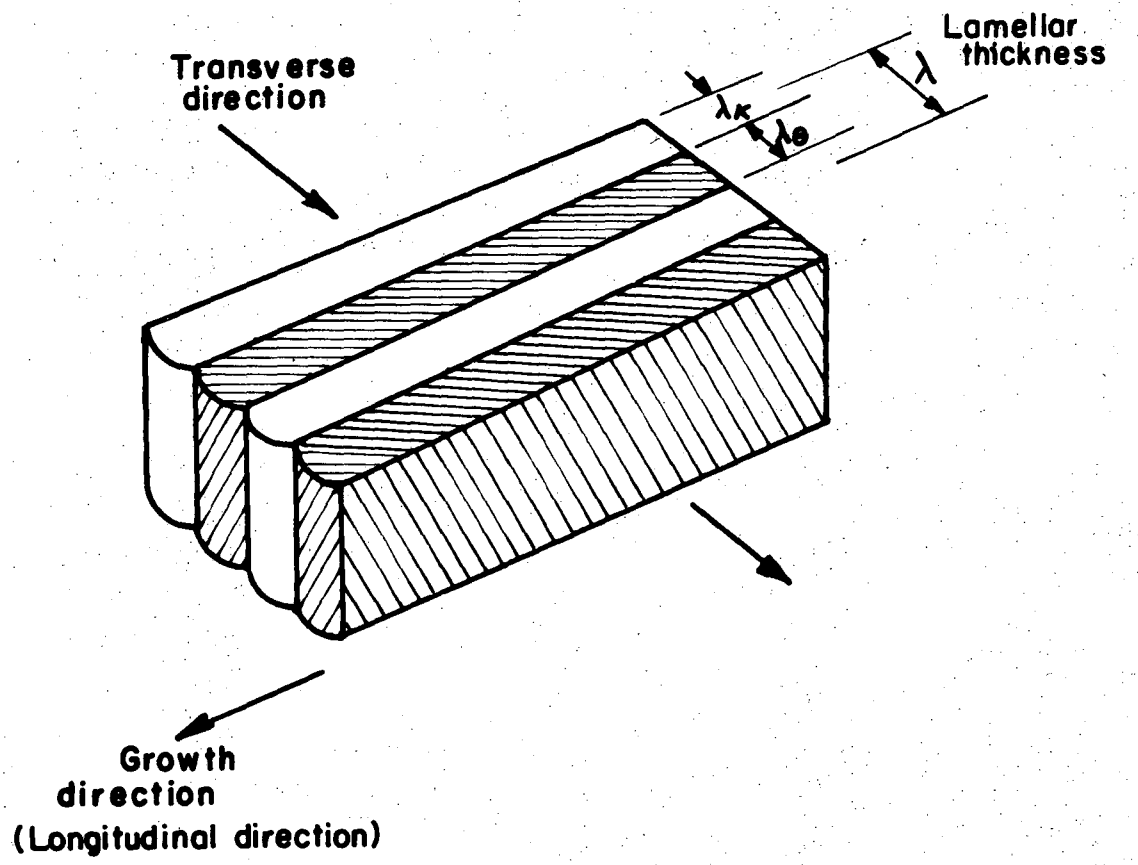
Lamellar thickness
λ
λκ
λe
Transverse direction
Growth direction
(Longitudinal direction)
XBL 7412-7678

Fig. 2

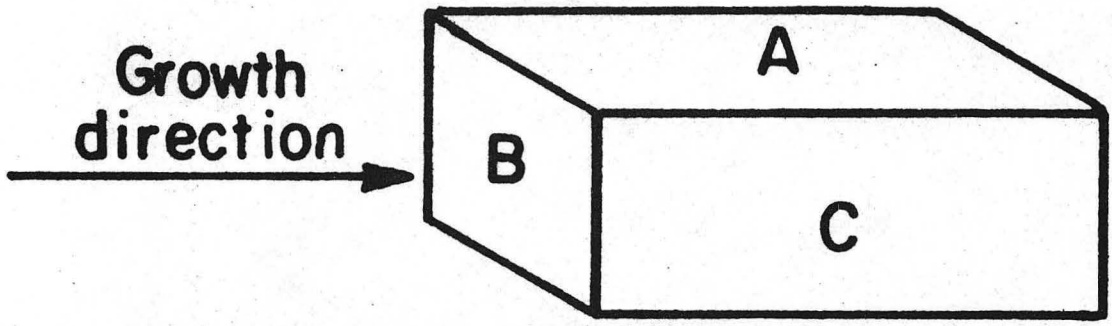

XBL 7412-7707

Fig. 3

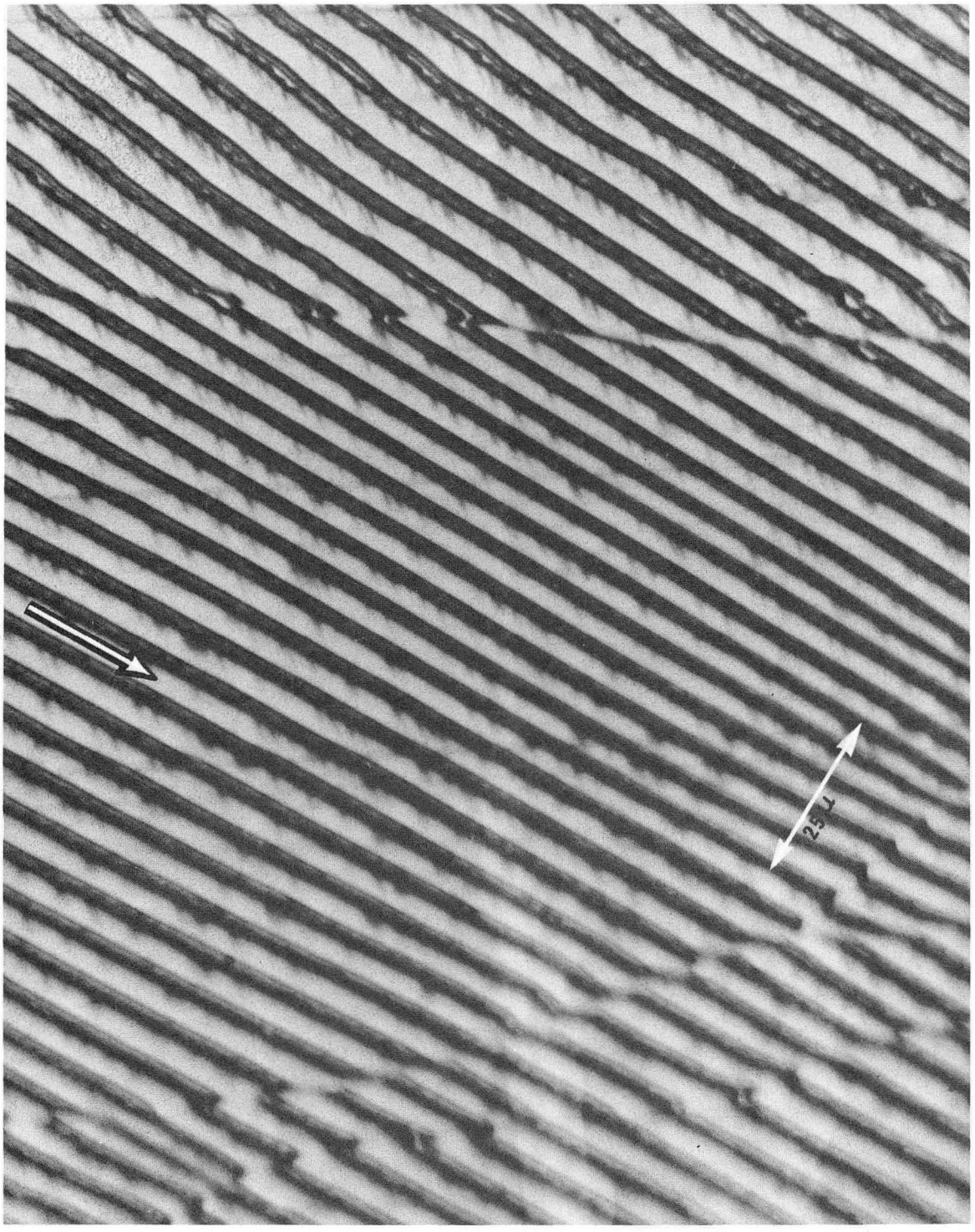

XBB 7412-8872

Fig. 4a

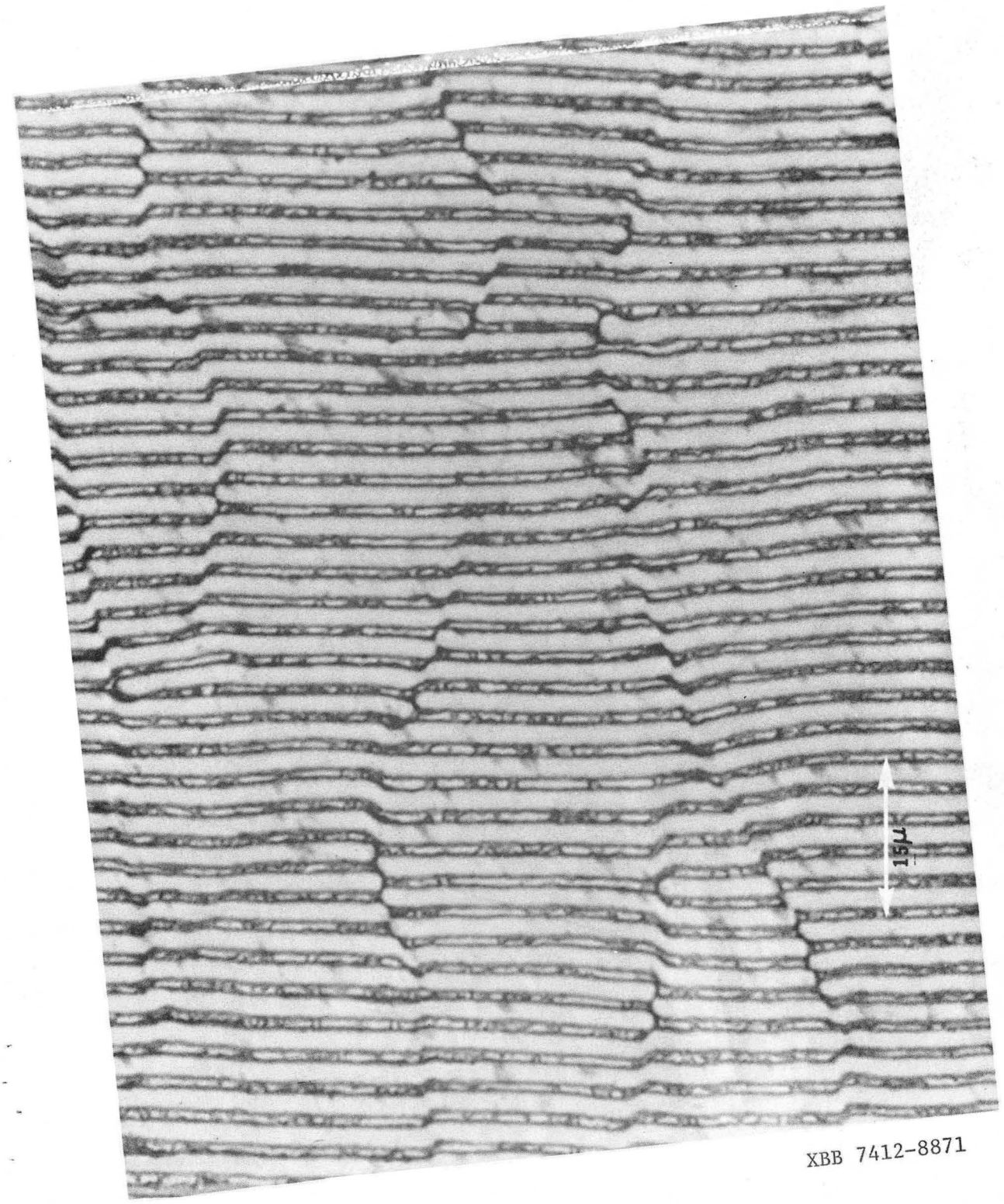

Fig. 4b

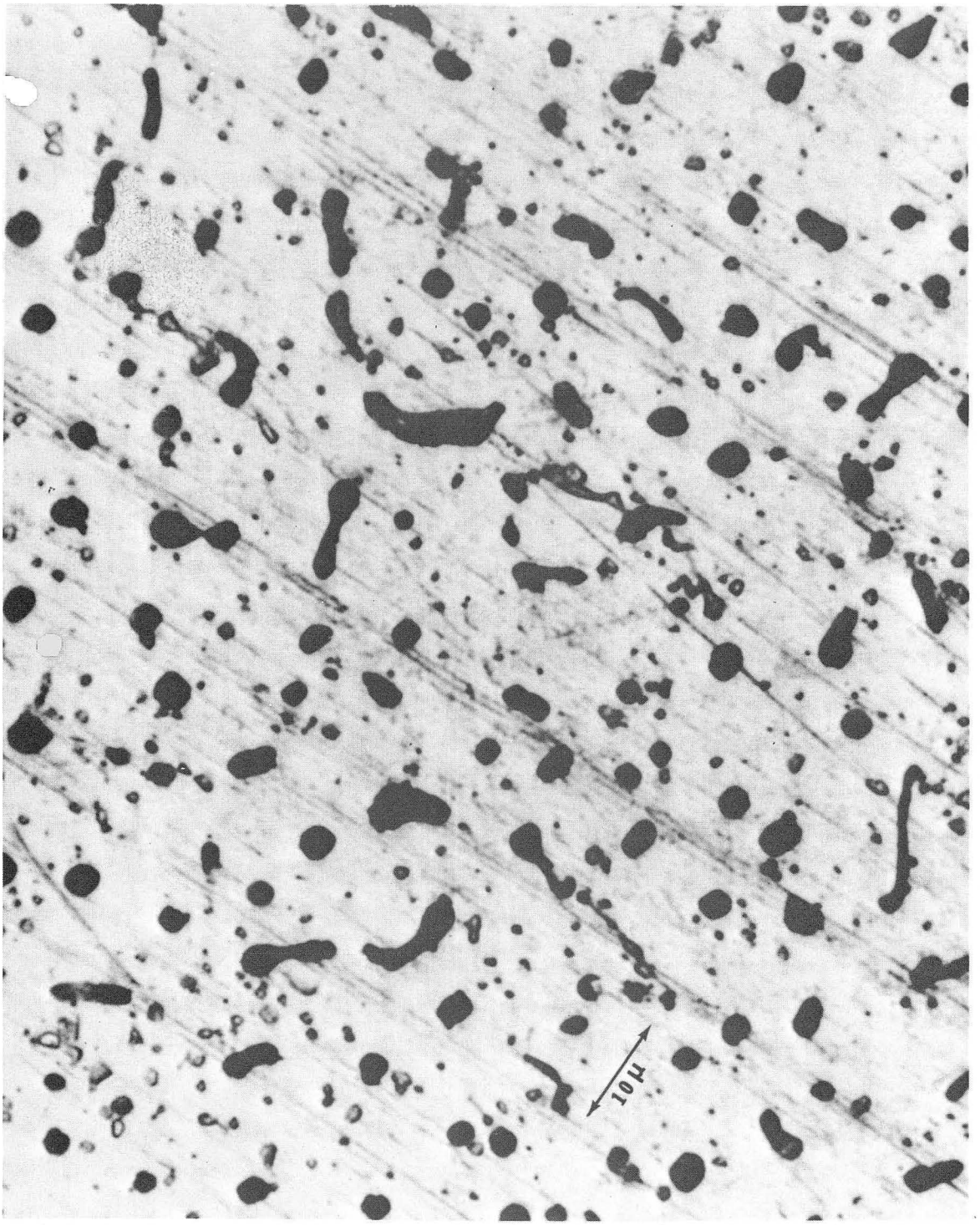

XBB 7412-8870

Fig. 5a

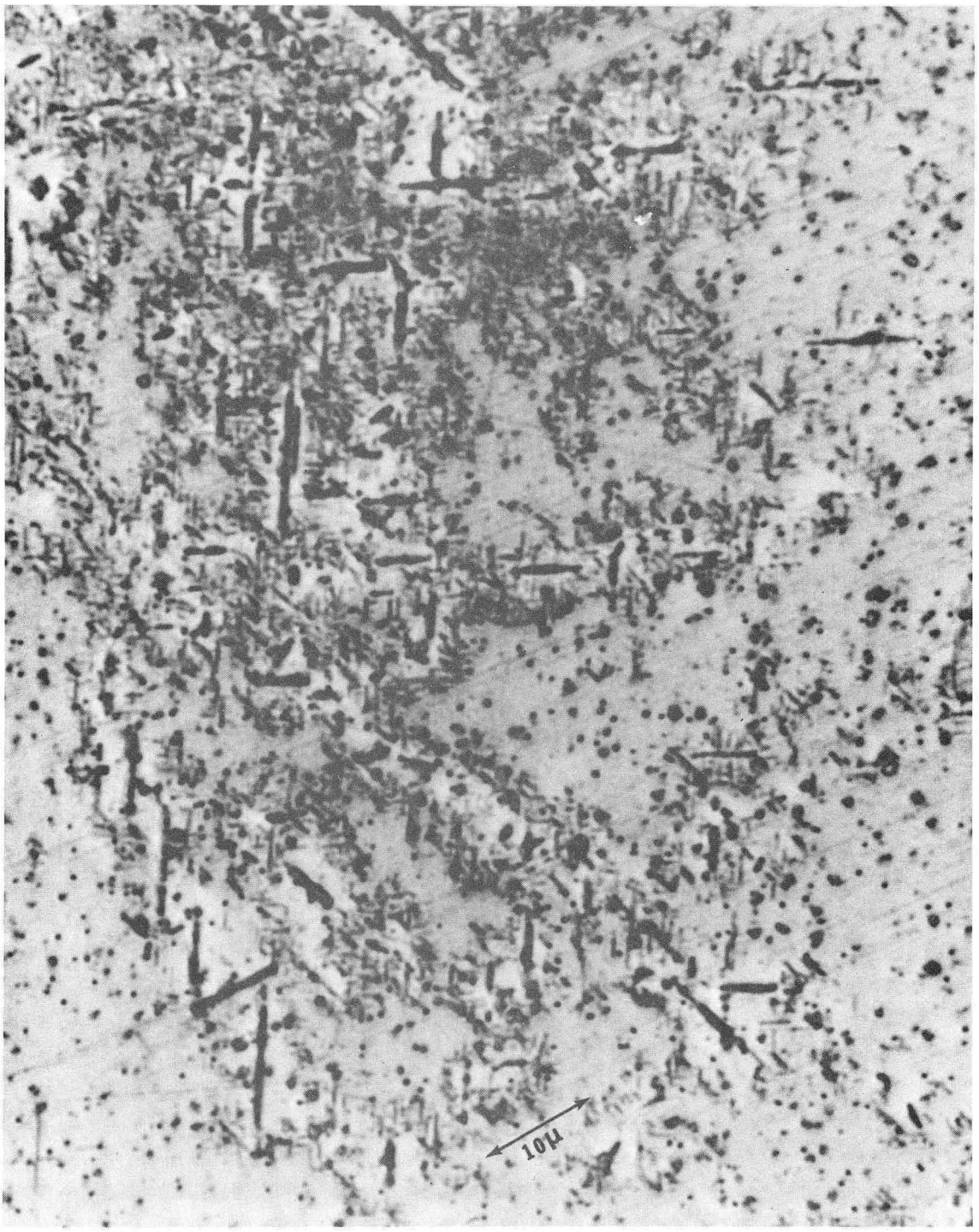

XBB 7412-8869

Fig. 5b

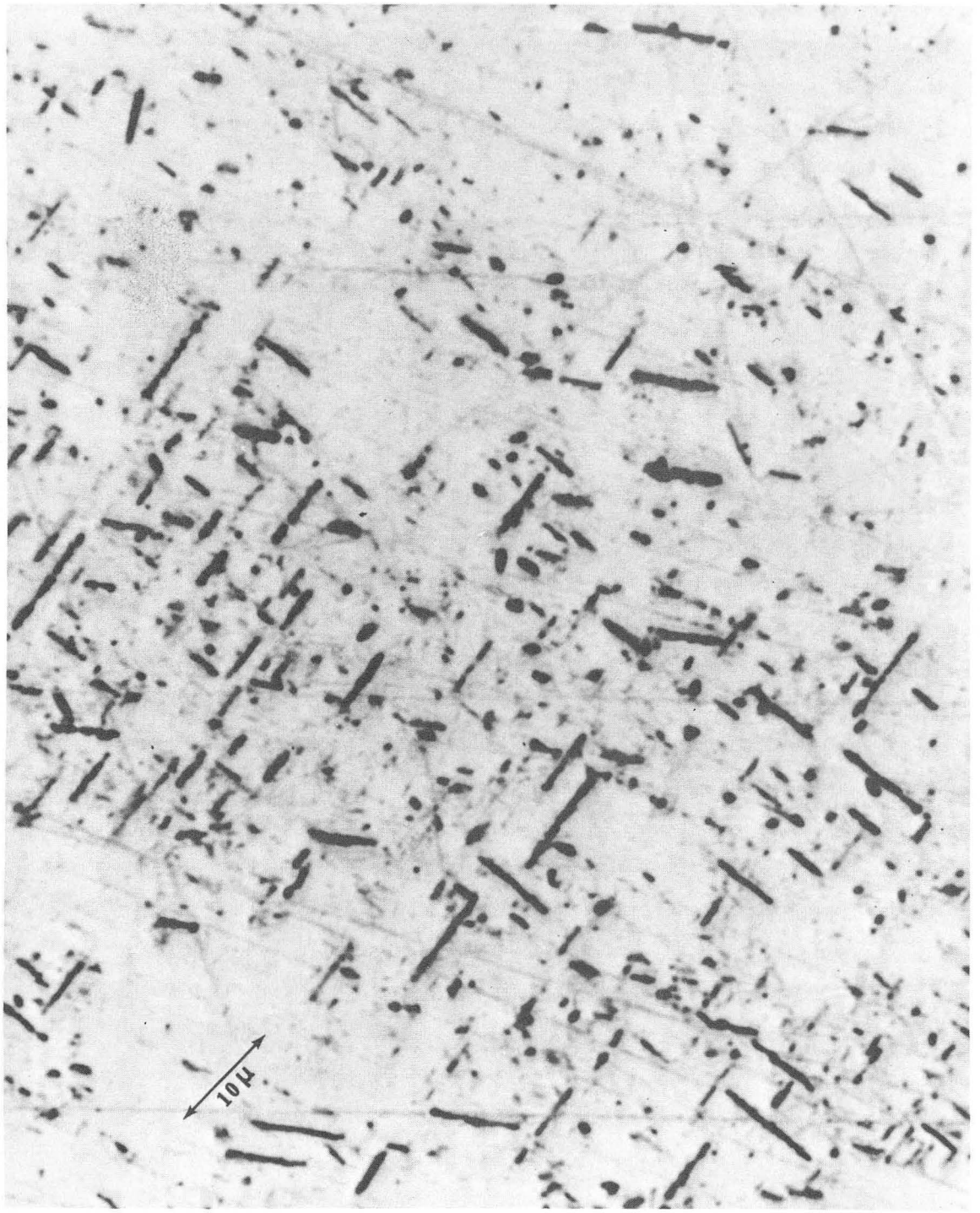

XBB 7412-8868

Fig. 5c

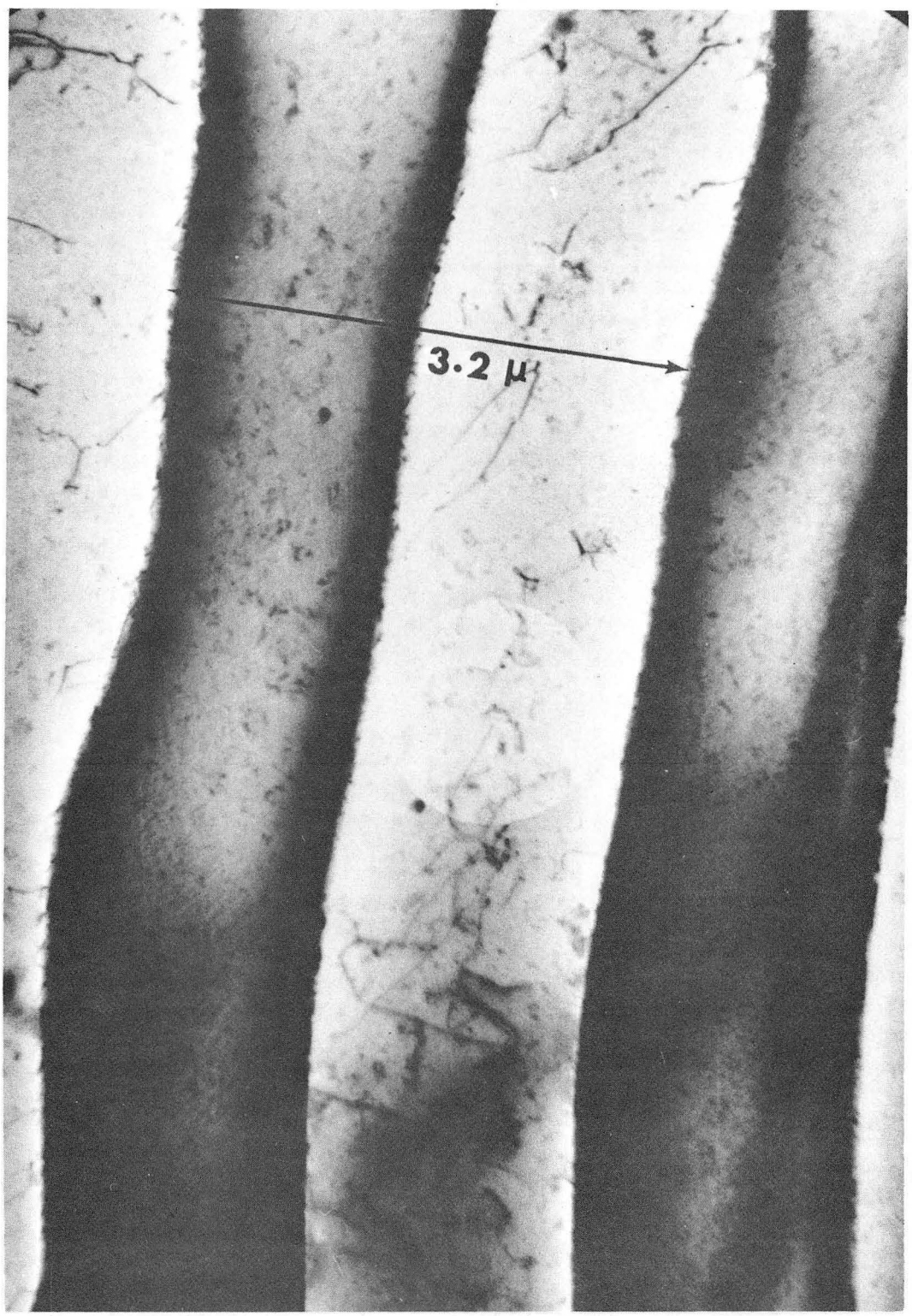

XBB 7412-8875

Fig. 6

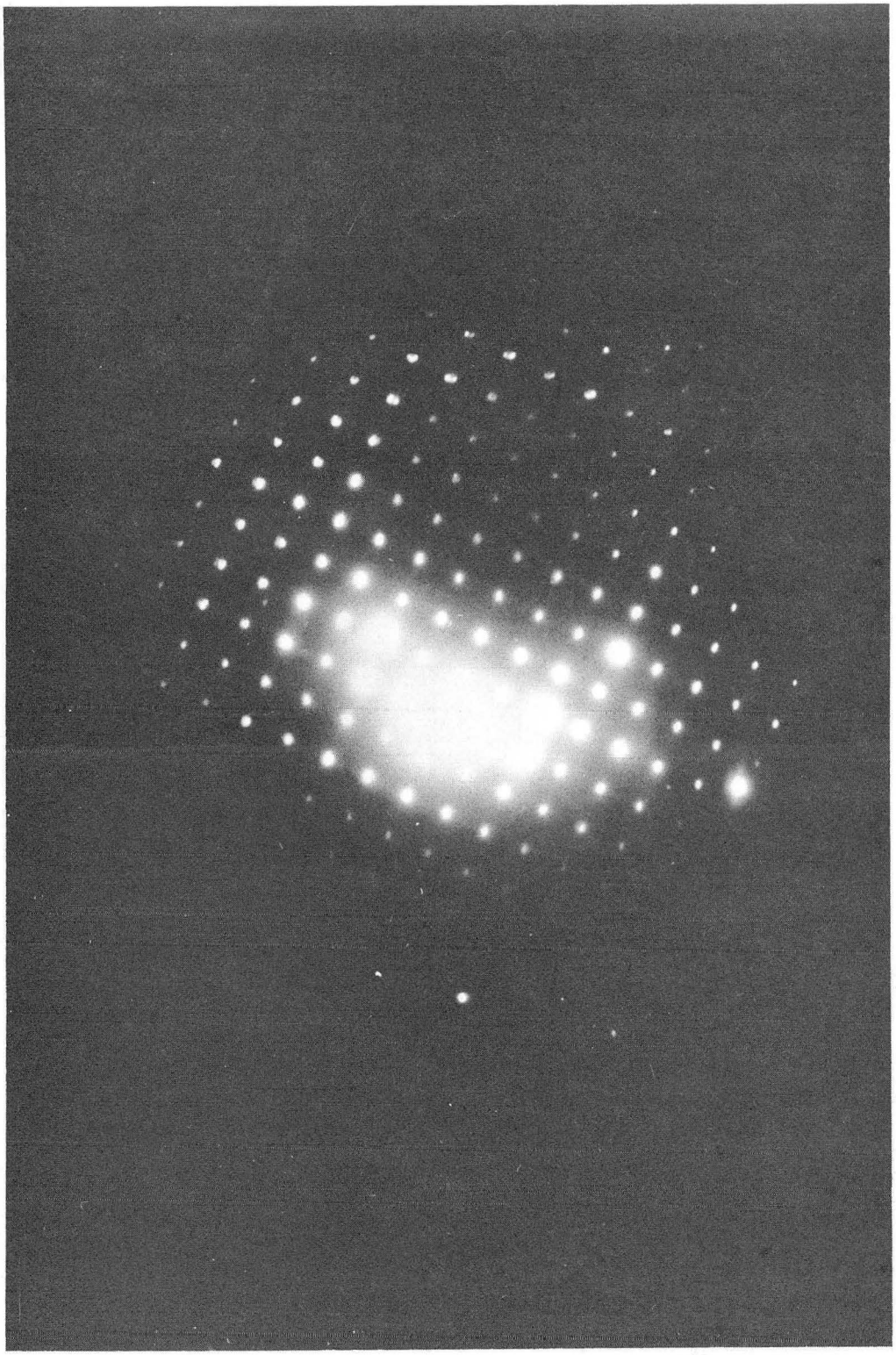

XBB 7412-8874

Fig. 7a

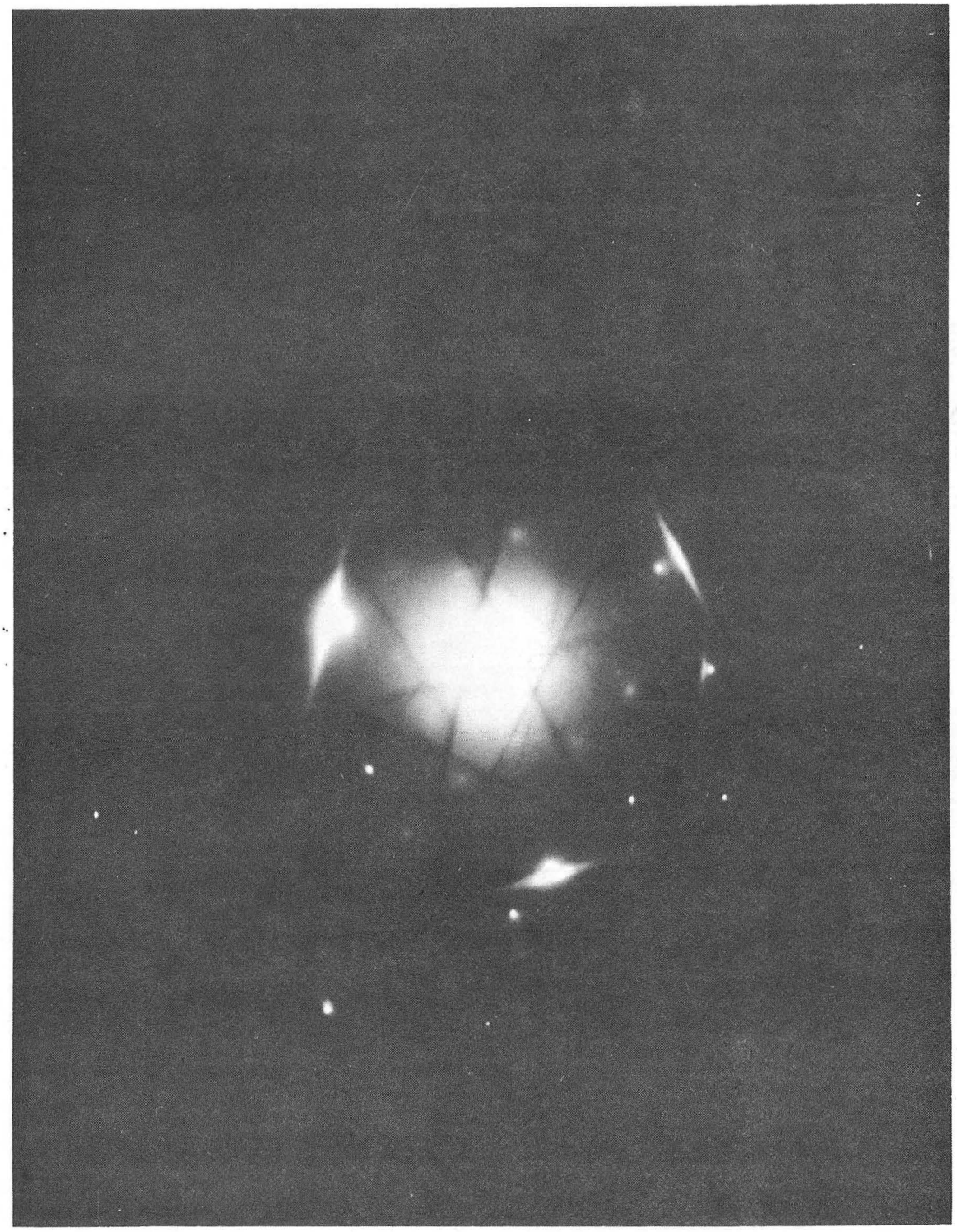

XBB 7412-8873

Fig. 7b

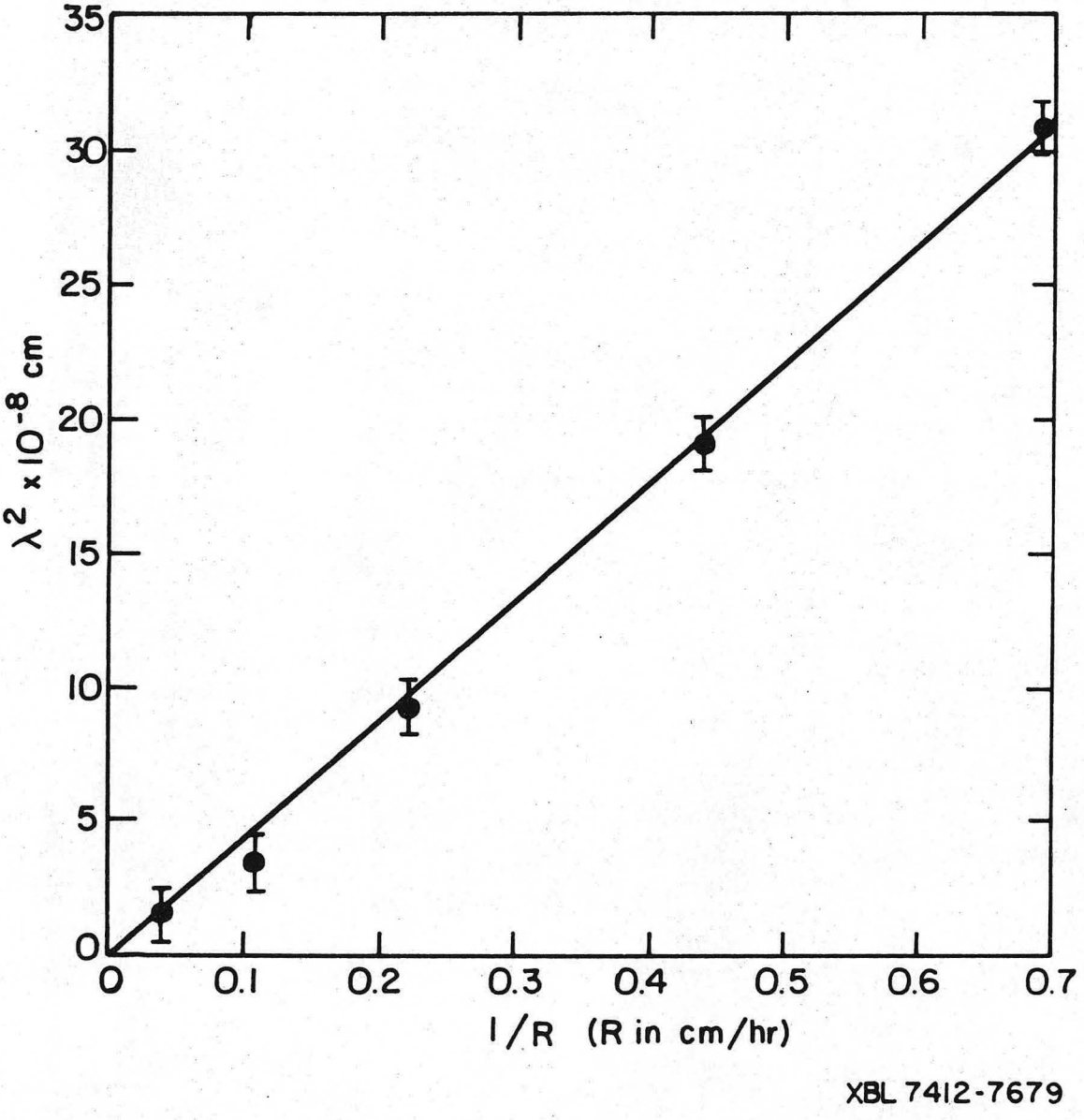
35
30
25
20
15
10
5
0
$\lambda^2 \times 10^{-8}$ cm
0
0.1
0.2
0.3
0.4
0.5
0.6
0.7
1/R (R in cm/hr)
XBL 7412-7679

Fig. 8

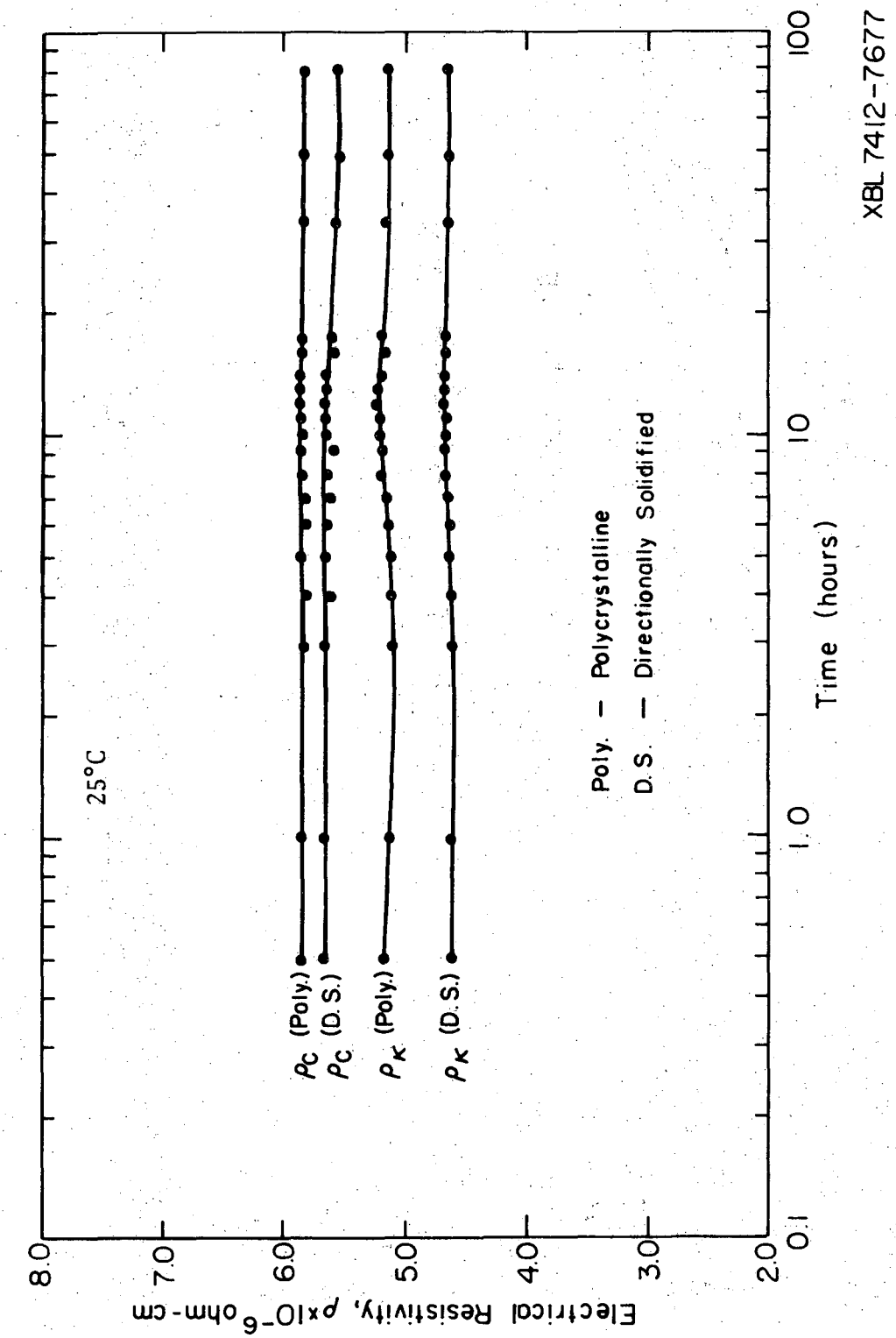

Fig. 9

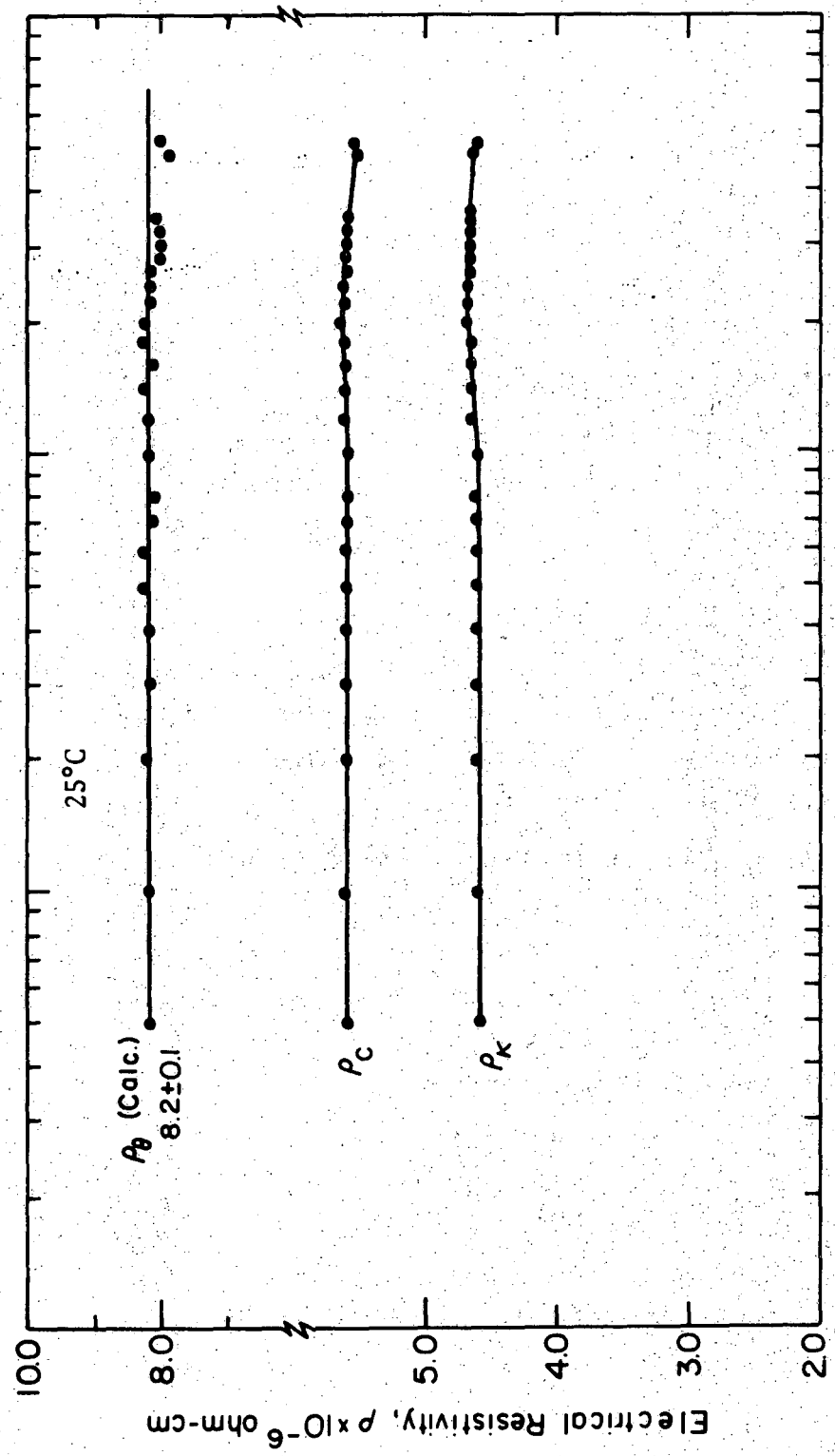

XBL 7412-7680

Fig. 10

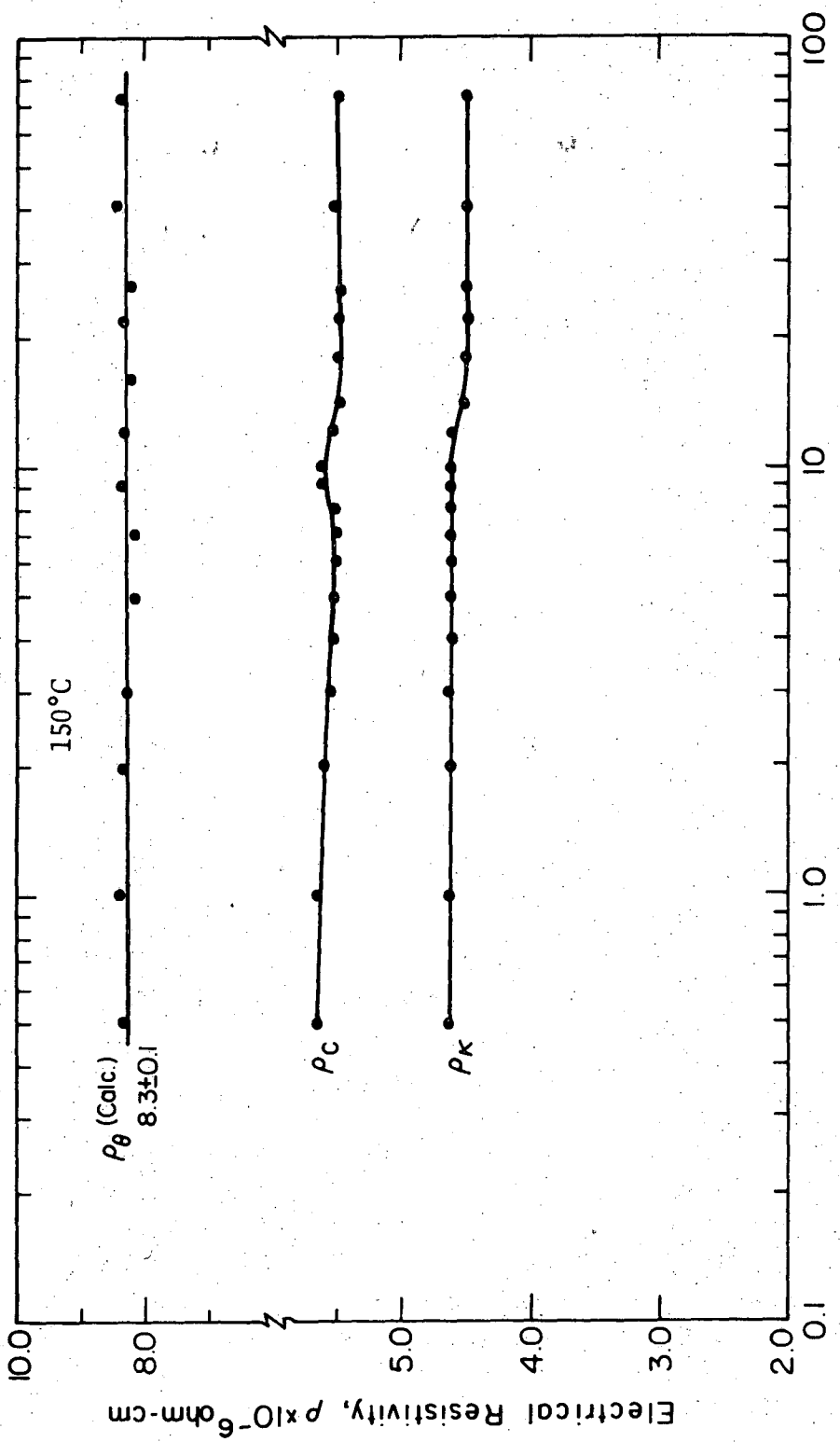

XBL 7412-7681

Fig. 11

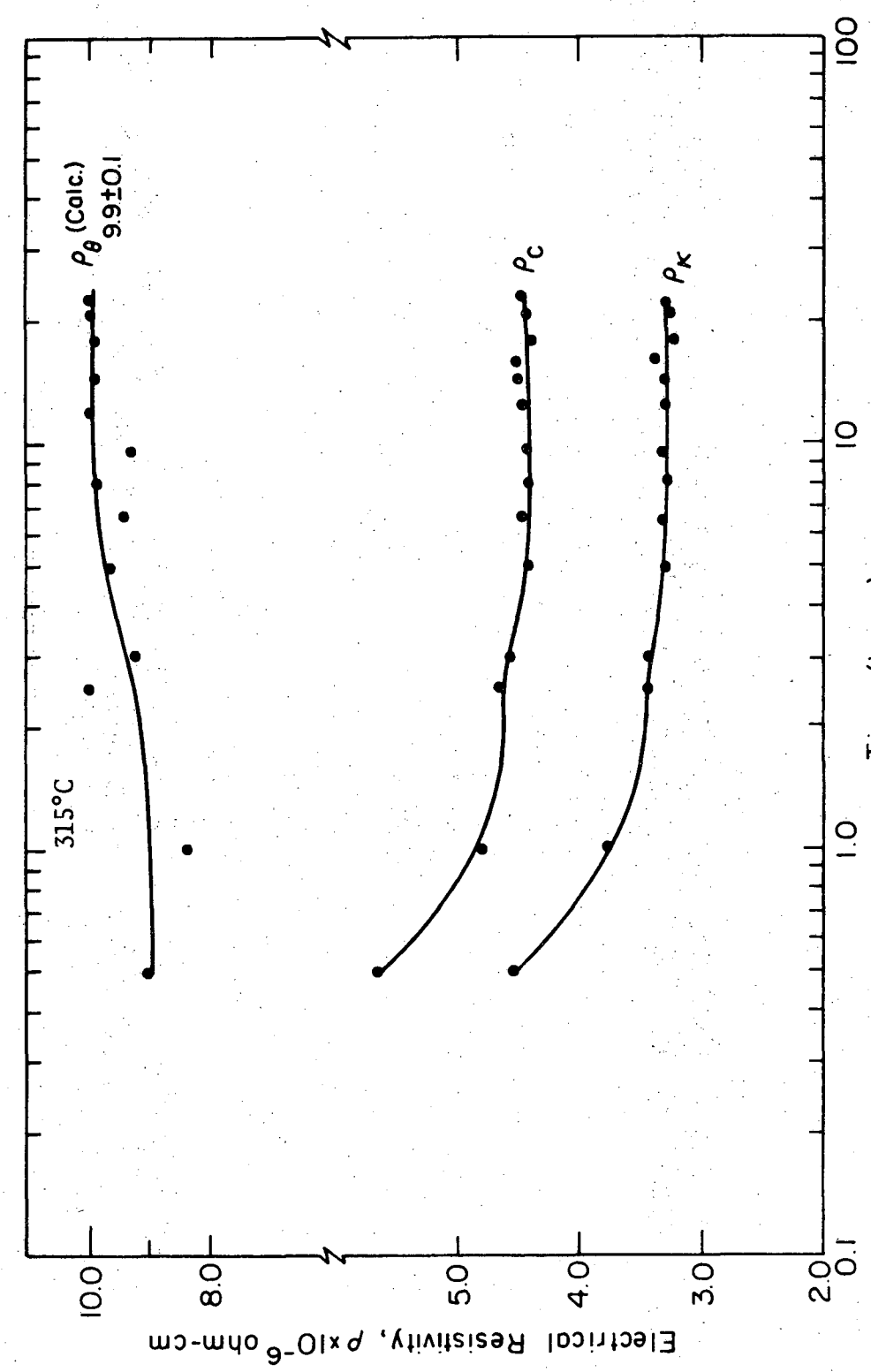
Electrical Resistivity, $\rho \times 10^{-6}$ ohm-cm
10.0
8.0
5.0
4.0
3.0
2.0
0.1
1.0
10
100
Time (hours)
315°C
ρ_θ (Calc.) 9.9±0.1
ρ_c
ρ_K
XBL 7412-7682

Fig. 12

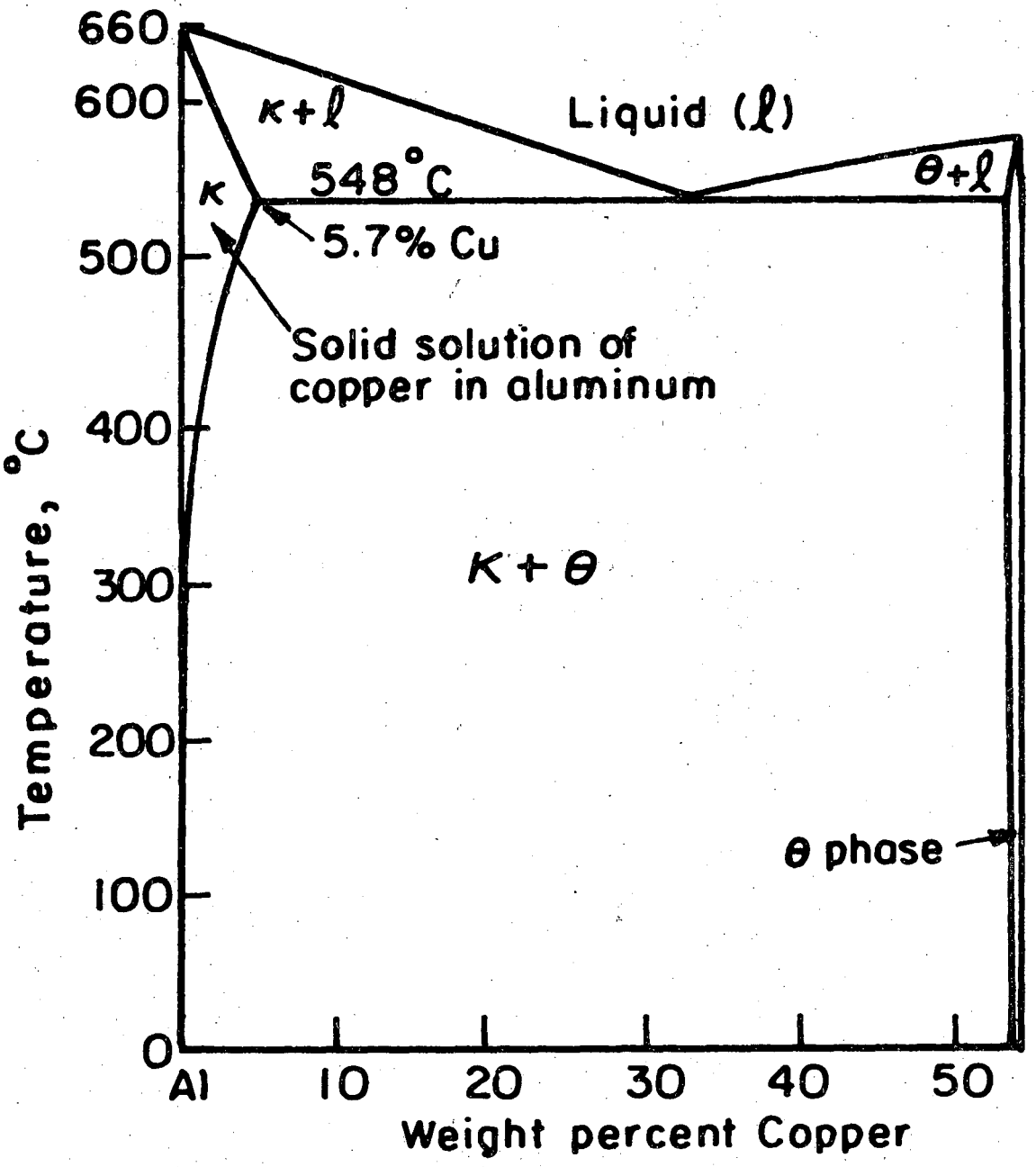

XBL 7412-7840

Fig. 13

TECHNICAL INFORMATION DIVISION
LAWRENCE BERKELEY LABORATORY
UNIVERSITY OF CALIFORNIA
BERKELEY, CALIFORNIA 94720